

# Detection of Iron Emission in the $z = 5.74$ QSO SDSSp J104433.04-012502.2 \*

Kentaro AOKI †

*Institute of Astronomy, School of Science, The University of Tokyo, Mitaka, Tokyo 181-0015*

*kaoki@ioa.s.u-tokyo.ac.jp*

Takashi MURAYAMA

*Astronomical Institute, Tohoku University, Aoba-ku, Sendai, Miyagi 980-8578*

*murayama@astr.tohoku.ac.jp*

and

Kiyomi DENDA

*National Astronomical Observatory of Japan, 2-21-1 Osawa, Mitaka, Tokyo 181-8588*

(Received 0 0; accepted 0 0)

## Abstract

We obtained near-infrared spectroscopy of the  $z=5.74$  QSO, SDSSp J104433.04-012502.2 with the Infrared Camera and Spectrograph of the Subaru telescope. The redshift of 5.74 corresponds to a cosmological age of 1.0 Gyr for the current  $\Lambda$ -dominated cosmology. We found a similar strength of the Fe II (3000-3500 Å) emission lines in SDSSp J104433.04-012502.2 as in low redshift QSOs. This is the highest redshift detection of iron. We subtracted a power-law continuum from the spectrum and fitted model Fe II emission and Balmer continuum. The rest equivalent width of Fe II (3000-3500 Å) is  $\sim 30$  Å which is similar to those of low redshift QSOs measured by the same manner. The chemical enrichment models that assume the life time of the progenitor of SNe Ia is longer than 1 Gyr predict that weaker Fe II emission than low redshift. However, none of the observed high redshift ( $z > 3$ ) QSOs show a systematic decrease of Fe II emission compared with low redshift QSOs. This may due to a shorter lifetime of SNe Ia in QSO nuclei than in the solar neighborhood. Another reason of strong Fe II emission at  $z = 5.74$  may be longer cosmological age due to smaller  $\Omega_M$ .

**Key words:** galaxies: active — galaxies: evolution — quasars: individual (SDSSp J104433.04-012502.2)

## 1. Introduction

The enrichment of  $\alpha$ -elements (e.g., O and Mg) in the universe has different time scales from that of iron-peak elements. While both  $\alpha$ -elements and iron are produced by SNe II, SNe Ia produce mostly iron. The progenitors of SNe Ia are intermediate mass stars in binary systems and have a lifetime of  $\sim 1$  Gyr although there is still debate on the progenitors of SNe Ia and their lifetime (e.g. Branch 1998 and Hillebrandt and Niemeyer 2000 for recent reviews). The 1 Gyr lifetime of the progenitors of SNe Ia is longer than those of SNe II, which are massive stars. The iron/alpha abundance ratio shows a rapid increase when SNe Ia start to explode. The  $[O/Fe] - [Fe/H]$  relation in the solar neighborhood is reproduced by that scenario assuming a 0.5-3 Gyr lifetime of the progenitors of SNe Ia (Yoshii et al. 1996; Kobayashi et al. 1998). Among high redshift objects, except for metal absorption-line systems, QSOs' spectra show both iron and  $\alpha$ -element spectral features. In particular, both Mg II  $\lambda 2798$  Å and Fe II

UV (2000-3000 Å) and Fe II (3000-3500 Å) emission-lines are emitted from the same ionized zone of the broad line region gas, and their similar wavelengths mean that extinction is similar. Therefore we can use the intensity ratio of their fluxes as an indicator of iron/alpha elements abundance ratios (Wills et al. 1985; Hamann & Ferland 1993). Comparison of the observed intensity ratio,  $I(\text{Fe II})/I(\text{Mg II})$ , in low redshift QSOs with results of model calculations of the broad line region suggests iron overabundance by a factor of  $\sim 3$  at low redshift (Wills et al. 1985). The iron overabundance of low redshift QSOs is reproduced by a QSO chemical enrichment model assuming rapid star formation and a delay of SNe Ia events (Hamann & Ferland 1993).

Recently, more than 20 high redshift ( $3.3 < z < 4.7$ ) QSOs have been observed with near-infrared spectroscopy and Mg II and Fe II UV and Fe II (3000-3500 Å) emission-lines were measured (Kawara et al. 1996; Murayama et al. 1999; Thompson et al. 1999; Dietrich and Hamann 2001; Dietrich et al. 2002). Their  $I(\text{Fe II (UV)})/I(\text{Mg II})$  are 7–10 and comparable to that of low redshift QSOs (Wills et al. 1985). These ratios are interpreted as suggesting QSO ages  $> 1$  Gyr in terms of the chemical enrichment model (Hamann & Ferland 1993; Yoshii et al. 1998). The chemical enrichment model (Yoshii et al.

\* Based on data collected at Subaru Telescope, which is operated by the National Astronomical Observatory of Japan.

† Present address: Subaru Telescope, National Astronomical Observatory of Japan, 650 North A'ohoku Place, Hilo, Hawaii 96720 U.S.A.

1998) indicates that the  $I(\text{Fe II (UV+optical)})/I(\text{Mg II})$  remains less than 2 until 1 Gyr has passed since first star formation occurred. After 1 Gyr has passed,  $I(\text{Fe II (UV+optical)})/I(\text{Mg II})$  rapidly increases to  $\sim 12$  at 1.5 Gyr. The highest redshift for which  $I(\text{Fe II})/I(\text{Mg II})$  was observed was 4.7 (Thompson et al. 1999; Dietrich and Hamann 2001) which corresponds to age of 1.3 Gyr in a cosmology with the current most likely cosmological parameters<sup>1</sup>. The large value of the  $I(\text{Fe II})/I(\text{Mg II})$  suggests that the first star formation occurred at  $z \gtrsim 10$  which corresponds to 0.5 Gyr (Dietrich and Hamann 2001).

The QSO at  $z = 5.74$ , SDSSp J104433.04-012502.2 (hereafter SDSS 1044-0125; Fan et al. 2000) was discovered in 2000 spring by the Sloan Digital Sky Survey (York et al. 2000). It is a luminous QSO ( $L_{\nu, 2500} = 5.2 \times 10^{31}$  erg  $\text{s}^{-1}$   $\text{Hz}^{-1}$ ) and the highest redshift object as of February 2001 when the observation was made. Maiolino et al (2001) have found a broad absorption line in its spectrum suggesting that heavy absorption by gas with a column density  $N_{\text{H}} > 10^{24}$   $\text{cm}^{-2}$  is the reason for its X-ray faintness (Brandt et al. 2001). Goodrich et al. (2001) made moderate resolution near infrared spectroscopy and revised the redshift to 5.74 measuring the peak of CIV emission-line. Since its redshift of 5.74 corresponds to a cosmological age of 1.0 Gyr, SDSS 1044-0125 is less than 1 Gyr old and the progenitor of SNe Ia in the QSO would not have exploded yet. The Fe II emission of SDSS 1044-0125 is expected to be weak. Mg II emission line is difficult to observe because it is redshifted to a spectral region of low atmospheric transparency.

## 2. Observations and Data Reduction

Near-infrared ( $J$ ,  $H$ , and  $K$  band) spectra of SDSS 1044-0125 were obtained with the Infrared Camera and Spectrograph (IRCS; Kobayashi et al. 2000) at the Cassegrain focus of the Subaru telescope on the nights of 2001 February 4 and 5 (UT). Both nights were photometric, but the seeing was unstable. It changed from  $0''.4$  to  $1''.2$  in  $K$  band. The projected pixel size of the  $1024^2$  ALADDIN II array was  $0''.058$  along the slit, and  $3.7$ ,  $4.7$  and  $6.1$   $\text{\AA}$  along the dispersion direction in  $J$ ,  $H$ , and  $K$  band, respectively. A slit width of  $0''.9$  was used resulting in resolutions in  $J$ ,  $H$ , and  $K$  band of 74, 117, and 198  $\text{\AA}$  FWHM, respectively. We obtained 12, 12 and 64 exposures, each 300 sec integration, in  $J$ ,  $H$ , and  $K$  band, respectively, shifting the position of the QSO along the slit at intervals of  $7''$  between each integration. Total integration times on the QSO were 3600, 3600, and 19200 sec in  $J$ ,  $H$ , and  $K$  band respectively. Observations of a nearby G5 star, HD 93019, were made before and after the observation of the QSO at approximately same airmass to correct the spectra for telluric absorption, and for flux calibration. The spectra of a halogen lamp and a Argon lamp were obtained for flat field and wavelength calibration, respectively.

Data were reduced using IRAF<sup>2</sup>. Dark frames of the same integration times as for the QSO and the star, HD 93019, were subtracted from the data frames. The following procedures were separately applied for each wavelength band. After masking of bad pixels, flat fielding was done with an averaged and normalized flat frame. Sky was removed by subtracting an adjacent exposure with the QSO in a different position along the slit. The sky-subtracted QSO frames at the same position along the slit but different airmass were averaged because the low S/N of a single frame hampered a check on whether telluric absorption features were removed. Although S/N of the QSO's spectra were improved due to averaging, the continuum of the QSO in the averaged frame was not bright enough to trace its position. Therefore we first traced the spectra of the telluric absorption correction star, HD 93019. This trace was used for extraction of the QSO's spectra and the comparison spectra. The extracted one dimensional comparison spectra were used for wavelength calibration of the QSO's extracted one dimensional spectra. After wavelength calibration of the one dimensional spectra, the spectra of the QSO at different position along the slit were combined to produce the QSO's spectrum in each wavelength band. The spectra of HD 93019 were extracted from the sky subtracted frames and wavelength calibrated using one dimensional extracted comparison spectra. The spectra of HD 93019 obtained at different position along the slit but same airmass were combined to give a spectrum at each airmass in each wavelength band. For relative flux calibration, we divided the spectra of HD 93019 by a 5560 K blackbody spectrum to make relative sensitivity functions including telluric absorption. Since the QSO spectra obtained at different airmasses were combined into a single spectrum, we averaged relative sensitivity functions at different airmasses to correct telluric absorption and instrument sensitivity. The S/N of the QSO spectra in  $J$ ,  $H$ , and  $K$  band are  $\sim 5$ ,  $\sim 2$ , and  $\sim 12$ , respectively.

The detector covered between 1.18 and 1.38  $\mu\text{m}$  in  $J$  band, however, the sensitivity of the grism used was low shortward of 1.24  $\mu\text{m}$  and longward of 1.35  $\mu\text{m}$  and the signal from the QSO in that wavelength range was almost nothing. We therefore use the region between 1.24  $\mu\text{m}$  and 1.35  $\mu\text{m}$  for the  $J$  band spectrum.

## 3. Results

Figure 1 shows the rest-frame spectra of SDSS 1044-0125 in  $J$  and  $K$  band together with the spectra obtained by Maiolino et al. (2001). The spectra of SDSS 1044-0125 were deredshifted by adopting  $z=5.74$  (Goodrich et al. 2001) and were smoothed 4.8  $\text{\AA}$  in  $J$ , 13.5  $\text{\AA}$  in  $K$  band, respectively. Since our spectra were obtained under unstable seeing conditions, light from the QSO falling into

<sup>1</sup> We adopt  $\Omega_{\text{M}} = 0.3, \Omega_{\Lambda} = 0.7, H_0 = 65$   $\text{km s}^{-1}$   $\text{Mpc}^{-1}$  throughout the paper (Schmidt et al. 1998; Perlmutter et al. 1999; de Bernardis et al. 2000; Melchiorri et al. 2000).

<sup>2</sup> Image Reduction and Analysis Facility (IRAF) is distributed by the National Optical Astronomy Observatories, which are operated by the Association of Universities for Research in Astronomy, Inc., under cooperative agreement with the National Science Foundation.

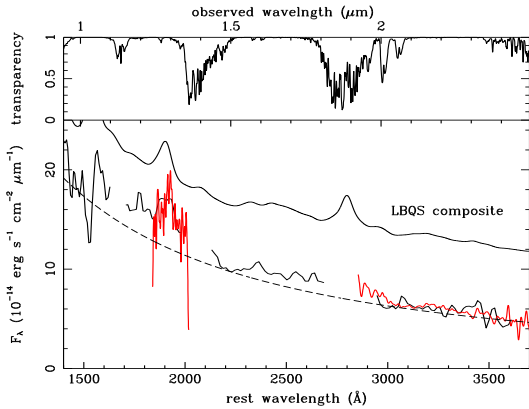


**Fig. 1.** (Upper panel) The atmospheric transmission curve. These data, produced using the program IRTRANS4, were obtained from the UKIRT www page. (Lower panel) Our spectra of SDSS 1044-0125, which is smoothed and shifted to the rest wavelength by the redshift of 5.74 (red line) and the reslut by Maiolino et al. (black line). The  $F_{\lambda}$  scale of our SDSS 1044-0125 spectra is shifted to the spectra obtained by Maiolino et al. (2001). The smoothed LBQS composite spectrum is plotted for comparison. It is shifted for clarity by 8. The dashed line is a power-law continuum ( $F_{\nu} \propto \nu^{-\alpha}$ ) with  $\alpha=0.54$ . See text for details.

the 0''9 slit varied among the exposures. The absolute flux density scale of the  $J$  band to  $K$  band spectrum is unknown. Maiolino et al. (2001) simultaneously obtained  $J$ ,  $H$ , and  $K$  band spectra of SDSS 1044-0125. We scaled our  $J$  and  $K$  band spectra to the spectra from Maiolino et al. (2001) at 1850-1965 Å in  $J$  band and 3000-3500 Å in  $K$  band, respectively. A emission feature is recognized at 1900 Å in the rest frame. This feature is a complex of Si III] and C III] as found by Maiolino et al. (2001). Since our  $H$  band spectrum of SDSS 1044-0125 is very low S/N, we do not use the  $H$  band data. As shown by Maiolino et al. (2001), the spectra of SDSS 1044-012 is similar to the Large Bright Quasar Survey (LBQS) composite spectrum<sup>3</sup> using total data set (Brotherton et al. 2001), which is a low redshift optically selected QSO template. The spectrum of SDSS 1044-0125 between 2900 Å and 3400 Å is similar to the LBQS composite spectrum. The bump between 2900 Å and 3000 Å is Fe II emission (Vestergaard and Wilkes 2001) and increase of flux from 3000 Å to 3400 Å is also due to Fe II emission and the Balmer continuum (Wills et al. 1985; Verner et al. 1999).

We measured Fe II emission-line strength as follows. Since our spectrum covers limited wavelength range, we determined the power-law continuum ( $F_{\nu} \propto \nu^{-\alpha}$ ) at 1465 Å and 2231 Å in the spectrum of Maiolino et al. (2001). After subtracting the power-law continuum from the  $K$  band spectrum of SDSS 1044-0125, we assume that the SDSS1044-0125 spectrum can be fitted with a Fe II template and the Balmer continuum, so that

$$F_{\lambda,SDSS} = aF_{\lambda,FeII} + bF_{\lambda,Balmer\ continuum}.$$

We have done  $\chi^2$  fitting between 2855 Å, which is the

<sup>3</sup> <http://sundog.stsci.edu/first/QSOComposites/>

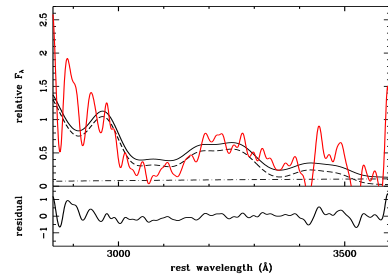


**Fig. 2.** The best fit result. The SDSS 1044-0125 spectrum with the power-law continuum subtracted is shown in a red line. The Fe II model template smoothed with 6000 km/s FWHM and a Balmer continuum are shown with a dashed line and a dot-dashed line, respectively. The Fe II plus a Balmer continuum is shown in a black solid line.

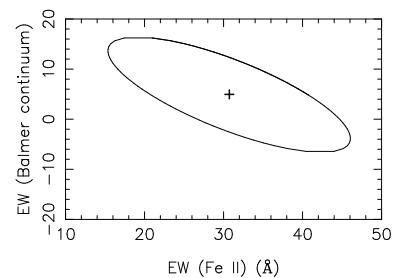


**Fig. 3.** The 68% confidence ellipse for the fit. The ordinate is rest frame EW of the Balmer continuum between 1000 Å and 3650 Å which is calculated from the scaling parameter  $b$ , the abscissa is the EW of the Fe II emission between 3000 Å and 3500 Å, which is calculated from the scaling parameter  $a$ . The crosses indicate the best fit value of EW.

shortest end of the  $K$  band spectrum, and 3600 Å, and derived the scaling parameter,  $a$  and  $b$ . The Fe II template was adopted from Wills et al. (1985). It was calculated assuming the hydrogen density,  $n_H = 10^{9.5} \text{ cm}^{-3}$ , the ionization parameter,  $U_{1Ryd} = 1.2 \times 10^8 \text{ cm sec}^{-1}$ . The optical depth at 2343 Å,  $\tau(2343) \times$  the turbulent velocity,  $V_t$  was assumed to be constant. We choosed the template under the condition of  $\tau(2343) = 5 \times 10^4$  and  $V_t = 7 \text{ km sec}^{-1}$  because the relative strength between Fe II multiplets were the most similar to the data of SDSS 1044-0125 among the templates available. We broadened the Fe II template by convolving it with a Gaussian of FWHM=6000 km  $\text{sec}^{-1}$  which is the line width of the C IV emission-line (Goodrich et al. 2001). The Balmer continuum assumed was a partially optical thick case given by Grandi (1982), with  $\tau_{BE} = 1.0$ ,  $\nu_{BE} = 3646 \text{ \AA}$  and  $T = 10000 \text{ K}$ ,

$$F_{\nu} \propto B_{\nu}(T)(1 - e^{-\tau}) \text{ with } \tau = \tau_{BE}(\nu/\nu_{BE})^{-3}.$$

The best fit results are shown in Figure 2 and in Table 1. The 68% ( $\sim 1\sigma$ ) confidence ellipses are also shown in Figure 3.

Combined with the power-law continuum flux at 3250 Å, the rest equivalent width (EW) of Fe II (3000 - 3500 Å) is  $\sim 30 \text{ \AA}$ . There is a possibility of contamination of O III fluorescence line  $\lambda 3133$  and He II  $\lambda 3203$ . If the significant emission of O III  $\lambda 3133$  existed, a 3200 Å bump

**Table 1.** The Result of Fit

$\alpha$	$\chi^2$ (d.o.f.)	Fe II <sup>a</sup> (rest EW (Å))
0.54	210 (52)	31±15

<sup>a</sup> Fe II is measured between 3000 and 3500 Å.

of the QSO would start  $\sim 50$  Å shorter wavelength than the spectra of the SDSS 1044-0125. We judged no significant contamination of O III fluorescence line. We could not estimate of He II  $\lambda 3203$ . The residual at 3200 Å may be He II (Fig.2). However, a dip at 3300 Å is not reproduced by only He II  $\lambda 3203$ , therefore we think that most of a bump between 3100 and 3400 Å is Fe II emission. We also measured Fe II strength of LBQS composite spectrum and the composite quasar spectrum from the Sloan Digital Sky Survey (SDSS) (Vanden Berk et al. 2001) with the same manner as for SDSS 1044-0125. The power-law continua were decided at the minimum between 1450 and 1470 Å and the minimum between 2200 and 2250 Å. The indexes of power-law continuum for LBQS and SDSS composites are 0.48 and 0.56, respectively. We have done  $\chi^2$  fitting between 2855 and 3600 Å using the same Fe II template and the Balmer continuum using for SDSS 1044-0125. The derived Fe II (3000 - 3500 Å) EW of LBQS composite and that of SDSS composite are 32 Å and 34 Å, respectively. This value is same as that of SDSS 1044-0125, so the strength of Fe II (3000 - 3500 Å) in SDSS 1044-0125 is similar to that of low redshift QSOs.

#### 4. Discussion

We could not observe the Mg II  $\lambda 2798$  emission line, however, N V, C IV, and C III] emission-line strength in SDSS 1044-0125 are similar to low redshift QSOs (Goodrich et al. 2001; Maiolino et al. 2001). This fact suggests the strength of Mg II of SDSS 1044-0125 will be also similar to that of low redshift QSOs. We measured the intensity of the Mg II emission line in LBQS composite and SDSS composite. The  $I(\text{Fe II (3000-3500 Å)})/I(\text{Mg II})$  in LBQS composite and SDSS composite are 0.69 and 0.70, respectively. Although we assume the strength of Mg II of SDSS 1044-0125 will be similar to that of low redshift QSOs and there is 50% error in the measurement of Fe II of SDSS 1044-0125, the  $I(\text{Fe II (3000-3500 Å)})/I(\text{Mg II})$  in SDSS 1044-0125 will be similar at least or larger than the result (0.15-0.4) from solar abundance Broad Line Region model calculation (Wills et al. 1985). Since the redshift of 5.74 corresponds to only 1.0 Gyr past from the Big Bang, iron abundance of the QSO is predicted to be solar value assuming high star formation efficiency (Hamann & Ferland 1993; Yoshii et al. 1998) which can reproduce  $I(\text{N V}) / I(\text{He II})$  in high redshift QSOs (Hamann and Ferland 1993) and iron overabundance in low redshift QSOs. Fe II emission in SDSS 1044-0125 is factor  $\sim 2$  stronger than the prediction by the chemical enrichment model of QSOs. These chemical enrichment models assume the typical lifetime of the progenitor of SNe Ia is more than 1 Gyr, therefore iron enrichment

relative to  $\alpha$ -element delays. The 0.5-3 Gyr lifetime of the progenitor of SNe Ia naturally explains the [O/Fe] - [Fe/H] relation in the solar neighborhood (Yoshii et al. 1996; Kobayashi et al. 1998), however, the lifetime of the progenitor of SNe Ia is not theoretically constrained so much because the lifetime of the companion in case of a white dwarf model accreting from the matter from the companion or intrinsic separation in case of merging white dwarfs model (Iben, & Tutukov 1984; Tutukov & Yungelson 1994) is unknown. The merging white dwarf model predicts shorter lifetime (0.3 - 0.4 Gyr) of the progenitor (Tutukov & Yungelson 1994). All observed high redshift ( $z > 3$ ) QSOs which are all luminous one and must be massive galaxy have similar  $I(\text{Fe II})/I(\text{Mg II})$  ratio to low redshift QSOs and no systematic decrease from them (Kawara et al. 1996; Murayama et al. 1999; Thompson et al. 1999; Dietrich and Hamann 2001; Dietrich et al. 2002). This line ratio suggests iron overabundance even if the age of universe  $\sim 1$  Gyr although there might be hidden physics which control Fe II emission line strength to be constant otherwise abundance change. The progenitor of SNe Ia in the nucleus of QSOs where gravitational potential is deeper and star density is higher may be different from that in the solar neighborhood (Thompson et al. 1999).

Another interpretation of strong Fe II emission at  $z = 5.74$  is different cosmological parameters from those we adopted. The relation of age and redshift depends on the cosmological parameters, the Hubble constant  $H_0$ , and the matter density  $\Omega_M$ . In a flat universe the age  $t \propto H_0^{-1} \Omega_M^{-1/2}$  at high redshift regime ( $z > 3$ ). If we assume  $H_0$  to be 50 km sec<sup>-1</sup> Mpc<sup>-1</sup>, the cosmological age at  $z = 5.74$  will be 1.4 Gyr which is consistent with the model predicts iron overabundance (Yoshii et al. 1998). The  $H_0$  of 50, however, is too small than that derived from such as Cepheid distance, Tully-Fisher relation, fundamental plane of elliptical galaxies, surface brightness fluctuations and SNe Ia (Mould et al. 2000). The estimate of the matter density  $\Omega_M$ , on the other hand, has rather large uncertainty. The measurement of inhomogeneity of the cosmic background radiation (de Bernardis et al. 2000; Melchiorri et al. 2000) and observations of high redshift SNe Ia (Schmidt et al. 1998; Permuter et al. 1999) indicate that a flat universe and  $0.1 \lesssim \Omega_M \lesssim 0.4$  (de Bernardis et al. 2000). If we adopt  $\Omega_M$  of 0.2 instead of 0.3, the cosmological age at  $z = 5.74$  will extends to 1.3 Gyr. The large  $I(\text{Fe II})/I(\text{Mg II})$  may suggest smaller  $\Omega_M$ .

#### 5. Conclusion

We obtained near-infrared spectroscopy of the  $z = 5.74$  QSO, SDSS 1044-0125 with the Infrared Camera and Spectrograph of the Subaru telescope. We found the strength of Fe II emission to be similar to low redshift QSOs. This is the highest redshift detection of iron. Its equivalent width of Fe II (3000-3500 Å) is  $\sim 30$  Å which is similar to those of low redshift QSOs. We estimated  $I(\text{Fe II 3000-3500 Å})/I(\text{Mg II}) \sim 0.7$ . Because the redshift of 5.74 corresponds to age of 1.0 Gyr in case of the



current  $\Lambda$ -dominated cosmological parameter, this ratio is larger than prediction of chemical enrichment models that assume the life time of the progenitor of SN Ia is longer than 1 Gyr. There is no systematic decrease of Fe II emission in observed high redshift QSOs ( $z > 3$ ) from low redshift ones. This suggests short lived SNe Ia progenitors may be more common in QSO nucleus than in the solar neighborhood. It is necessary to search whether there is no hidden physics of Fe II emission mechanism in order to show definitely the possibility of short-lived SNe Ia progenitors. Another interpretation of high  $I(\text{Fe II})/I(\text{Mg II})$  at  $z = 5.74$  is smaller  $\Omega_M$  than we adopt. The cosmological age at  $z = 5.74$  may be longer than 1 Gyr.

We are grateful to the IRCS instrument team, especially H. Terada and N. Kobayashi for their help and valuable comments during our observations. We also thank B. Wills for kindly providing an Fe II model template, her valuable comments, and improving the English expression. Discussions with M. Yoshida, T. Yamada, and N. Arimoto have improved this paper. The data reduction was done using the facilities of the Astronomical Data Analysis Center, National Astronomical Observatory of Japan, which is an inter-university research institute operated by the Ministry of Education, Culture, Sports, Science and Technology. This work was financially supported in part by Grant-in-Aids for the Scientific Research (No. 13740122) or the Japanese Ministry of Education, Culture, Sports, Science and Technology.

## References

- [Branch 1998] Branch, D. 1998, *ARA&A* 36, 17
- [Brandt et al.2001] Brandt, W. N., Guainazzi, M., Kaspi, S., Fan, X., Schneider, D. P., Strauss, M. A., Clavel, J., & Gunn, J. E. 2001, *AJ* 121, 591
- [Brotherton et al. 2001] Brotherton, M. S., Tran, H. D., Becker, R. H., Gregg, M. D., Laurent-Muehleisen, S. A., & White, R. L. 2001, *ApJ* 546, 775
- [de Bernardis et al. 2000] de Bernardis, P., Ade, P.A.R., Bock, J.J., Bond, J.R., Borrill, J., Boscaleri, A., Coble, K., Crill, B.P. et al. 2000, *Nature* 404, 955
- [Dietrich and Hamann 2001] Dietrich, M. & Hamann, F. 2001, in *Astrophysical Ages and Time Scales*, ed. T. von Hippel, C. Simpson, & N. Manset (San Francisco: ASP), 245, 575
- [Dietrich et al. 2002] Dietrich, M., Appenzeller, I., Vestergaard, M., & Wagner, S. J. 2002, *ApJ* 564, 581
- [Fan et al. 2000] Fan, X., White, R. L., Davis, M., Becker, R. H., Strauss, M. A., Haiman, Z., Schneider, D. P., Gregg, M. D., et al. 2000, *AJ* 120, 1167
- [Goodrich 2001] Goodrich, R., W., Campbell, R., Chaffee, F., Hill, G., M., Sprayberry, D., Brandt, W., N., Schneider, D., P., & Kaspi, S. et al. 2001, *ApJL* 561, L23
- [Grandi 1982] Grandi, S. A.. 1982, *ApJ* 255, 25
- [Hamann & Ferland 1993] Hamann, F., & Ferland, G. 1993, *ApJ* 418, 11
- [Hillebrandt and Niemeyer 2000] Hillebrandt, W. & Niemeyer, J. C. 2000, *ARA&A* 38, 191
- [Iben & Tutukov 1984] Iben, I. Jr., & Tutukov, A. V. 1984, *ApJS* 54, 335
- [Kawara et al. 1996] Kawara, K., Murayama, T., Taniguchi, Y., & Arimoto, N. 1996, *ApJL* 470, L85
- [Kobayashi et al. 1998] Kobayashi, C., Tsujimoto, T., Nomoto, K., Hachisu, I., & Kato, M. 1998, *ApJL* 503, L155
- [Kobayashi et al. 2000] Kobayashi N., Tokunaga, A., Terada, H., Goto, M., Weber, M., Potter, R., Onaka, P., Ching, G., et al. 2000, in *Optical and IR Telescope Instrumentation and Detectors*, ed. M. Iye, & A. F. Moorwood (Bellingham: SPIE), 1056
- [Maiolino et al. 2001] Maiolino, R., Mannucci, F., Baffa, C., Gennari, S., & Oliva, E. 2001, *A&A* 372, L5
- [Melchiorri et al. 2000] Melchiorri, A., Ade, P.A.R., de Bernardis, P., Bock, J.J., Borrill, J., Boscaleri, A., Crill, B.P., de Troia, G. et al. 2000, *ApJL* 536, L63
- [Mould et al. 2000] Mould, J.R., Huchra, J.P., Freedman, W.L., Kennicutt Jr., R.C., Ferrarese, L., Ford, H.C., Gibson, B.K., Graham, J.A., et al. 2000, *ApJ* 529, 786
- [Murayama et al. 1999] Murayama, T., Taniguchi, Y., Evans, A.S., Sanders, D. B., Hodapp, K.-W., Kawara, K., & Arimoto, N. 1999, *AJ* 117, 1645
- [Perlmutter et al. 1999] Perlmutter, S., Aldering, G., Goldhaber, G., Knop, R.A., Nugent, P., Castro, P.G., Deustua, S., Fabbro, S., et al. 1999, *ApJ* 517, 565
- [Schmidt et al. 1998] Schmidt, B.P., Suntzeff, N.B., Phillips, M.M., Schommer, R.A., Clocchiatti, A., Kirshner, R. P., Garnavich, P., Challis, P., et al. 1998, *ApJ* 507, 46
- [Thomson et al. 1999] Thompson, K.L., Hill, G. J., & Elston, R. 1999, *ApJ* 515, 487
- [Tutukov & Yungelson 1994] Tutukov, A. V., & Yungelson, L. R. *MNRAS* 268, 871
- [Vanden Berk et al. 2001] Vanden Berk, D. E., Richards, G., T., Bauer, A., Strauss, M. A., Schneider, D., P., Heckman, T. M., York, D. G., Hall, P. B. et al. 2001, *AJ* 122, 549
- [Verner et al. 1999] Verner, E.M., Verner, D.A., Korista, K.T., Ferguson, J.W., Hamann, F., and Ferland, G. 1999, *ApJS* 120, 101
- [Vestergaard and Wilkes 2001] Vestergaard, M. & Wilkes, B. J. 2001, *ApJS* 134, 1
- [Wills et al. 1985] Wills, B. J., Netzer, H. & Wills, D. 1985, *ApJ* 288, 94
- [York et al. 2000] York, D. G., Adelman, J., Anderson, Jr., J. E., Anderson, S. F., Annis, J., Bahcall N. A., Bakken, J. A., Barkhouser, R., et al. 2000, *AJ* 120, 1579
- [Yoshii et al. 1996] Yoshii, Y., Tsujimoto, T., & Nomoto, K. 1996, *ApJ* 462, 266
- [Yoshii et al. 1998] Yoshii, Y., Tsujimoto, T., & Kawara, K. 1998, *ApJL* 507, L113